

Rheology of 1-Butyl-3-Methylimidazolium Chloride Cellulose Solutions. I. Shear Rheology

R. J. Sammons,¹ J. R. Collier,² T. G. Rials,¹ S. Petrovan³

¹Forest Products Center, University of Tennessee, Knoxville, Tennessee 37996-4570

²Chemical and Biomedical Engineering, FAMU/FSU, Tallahassee, Florida 32320

³Chemical and Biomolecular Engineering Department, University of Tennessee, Knoxville, Tennessee 37996-2200

Received 15 November 2007; accepted 20 May 2008

DOI 10.1002/app.28733

Published online 10 July 2008 in Wiley InterScience (www.interscience.wiley.com).

ABSTRACT: In this article, shear rheology of solutions of different concentrations obtained by dissolution of cellulose in the ionic liquid (IL) solvent 1-butyl-3-methylimidazolium chloride ([Bmim]Cl) was studied by measuring the complex viscosity and dynamic moduli at different temperatures. The obtained viscosity curves were compared with those of lyocell solutions and melt blowing grade polypropylene melts of different melt flow rates (MFR). Master curves were generated for complex viscosity and dynamic moduli by using Carreau and Cross viscosity models to fit experi-

mental data. From the Arrhenius plots of the shift factors with respect to temperature, the activation energies for shear flow were determined. These varied between 18.99 and 24.09 kCal/mol, and were compared with values for lyocell solutions and different polymeric melts, such as polyolefins, polystyrene, and polycarbonate. © 2008 Wiley Periodicals, Inc. *J Appl Polym Sci* 110: 1175–1181, 2008

Key words: cellulose; ionic liquids; 1-butyl-3-methylimidazolium chloride; shear rheology; activation energy

INTRODUCTION

Cellulose is the most abundant natural, renewable, polymer that is used in the production of many materials. However, limited process ability due to dissolution difficulties has restricted its use in fibers, films, and other products. Many of the current processes involving cellulose use chemical reagents that contain sulfur, such as carbon disulfide in the viscose process, which is hazardous to the environment and humans even in reduced concentrations.¹ A new developing area of research deals with the cellulose processing by using environmentally benign solvents such as ionic liquids and *N*-methyl morpholine oxide (NMMO).

Literature is abundant with reports on cellulose dissolution and processing with different environmentally friendly solvents, including ILs, and we will mention but a few, because the main objective of this work is not an extensive review on this subject. Cellulose dissolution and the mechanism of the dissolution process have been studied by both experimental methods and computer modeling of the geometry and electronic structure of the solvent and its complexes with water and cellobiose.^{2–4} It was

found that dissolution can be done without activation or pretreatment in 1-butyl-3-methylimidazolium chloride ([Bmim]Cl) and regenerated from its solution. Degradation of cellulose in ionic liquids and preparation of some degraded cellulose products was also studied by Massonne et al.^{5,6} Codissolution in [Bmim]Cl and other solvents was carried out for the purpose of sensor development by encapsulating in a cellulose support and regeneration by precipitation.⁷ A new method for introducing enzymes into cellulosic matrices which can be formed into membranes, films, or beads has been developed using a cellulose-in-ionic-liquid dissolution and regeneration process.⁸ Mini- and extensive reviews were published on cellulose dissolution with ionic liquids or on applications of ionic liquids in carbohydrate chemistry.^{9,10} The molecular structure and synthesis of ILs most frequently employed in carbohydrate chemistry, the physicochemical properties of ILs that are relevant to the dissolution and functionalization of carbohydrates, and the mechanism of carbohydrate-IL interactions are discussed with an emphasis on imidazolium and pyridinium cations with different counterions. Finally, the very interesting novel applications of the solutions obtained are addressed, such as spinning of the dissolved biopolymer into fibers, extrusion into different shapes, formation of matrices and nanocomposites, and functionalization to produce derivatives.

There are few reports on characterization of cellulose solutions in ionic liquids, especially rheology

Correspondence to: J. R. Collier (john.collier@eng.fsu.edu).

Contract grant sponsor: EPA; contract grant number: R831658.

TABLE I
Thermal Properties of 1-butyl-3-methylimidazolium chloride, [Bmim]Cl

Melting point temperature (°C)	41
Glass transition temperature (°C)	-69
Start temperature of thermal decomposition temperature (°C)	150
Heat capacity @ 25°C (J mol ⁻¹ K ⁻¹)	322.7
Heat capacity @ 50°C (J mol ⁻¹ K ⁻¹)	333.7

studies. Dynamic moduli of an ionic liquid cellulose solution with different amounts of multiwalled-carbon-nanotubes were measured by Hao Zhang et al.¹¹ and rheological properties of wood and water washed steam exploded wheat straw pulps dissolved in [Bmim]Cl were studied by shear viscosity measurements.¹²

Both shear and elongational rheology are fundamental properties for polymer melts and solution processing. Extensional deformations play a significant role in many processing operations, which involve a rapid change of shape such as fiber spinning, film blowing, blow molding, and nonwoven melt processing.¹³

The objectives of this article, and the next in a series of three, is a systematic study of shear and elongational rheology of cellulose solutions in [Bmim]Cl. We have chosen this solvent because, as literature data show, it seems to be a good representative for ionic liquids used to do dissolution and processing of cellulose solutions.

EXPERIMENTAL

Materials

The cellulose used in this study was a dissolving pulp of degree of polymerization 670 (Buckeye Technologies Inc., Memphis, TN) and the IL used was [Bmim]Cl (Fisher, USA), the thermal properties being listed in Table I.¹⁴ Three cellulose/IL solutions of 8, 10, and 12% cellulose by weight were studied at the three temperatures of 80, 90, and 100°C.

Instruments and experimental technique

Dissolution of cellulose in the ionic liquid solvent was carried out in a Brabender internal mixer. Shear rheology measurements were done using the Advanced Rheometric Expansion System (ARES) rheometer (TA Instruments) and parallel plate geometry.

The sheets of dissolving pulp were ground to a fine powder and dried in an oven to constant weight. Ionic liquid [Bmim]Cl was melted first in the Brabender mixing chamber and then cellulose powder and propyl gallate (1% on cellulose) were added under continuous mixing at 90°C and 60

RPM rotors speed. Dissolution was performed until a clear viscous solution was obtained. The time of dissolution was different for different concentration solutions. After dissolution the samples were discharged from the mixing chamber into glass jars, sealed, and stored at room temperature for future testing.

The viscoelastic domain was tested by performing a dynamic strain sweep test, for each solution at the temperature of 90°C. Then the complex viscosity (η^*), as well as the dynamic moduli G' and G'' were measured by performing dynamic frequency sweep tests over an angular velocity range of 0.1–100 s⁻¹. To avoid water uptake by the sample while running the experiments, the edges of the specimen sandwiched between the plates were covered with a thin layer of a viscosity standard silicon oil (viscosity 29.1 Pa s at 25°C). All experiments were conducted at three temperatures of 80, 90, and 100°C. The zero-shear viscosity was determined by using the ORIGIN graphing software to fit complex viscosity data to Carreau or Cross models.

RESULTS AND DISCUSSION

Complex viscosity

Dynamic strain sweep test results are shown in Figure 1. Complex viscosity is constant on most of the tested strain range so that 1% strain was chosen for all dynamic frequency tests to measure complex viscosity and dynamic moduli. Figure 2 illustrates the effects of solution concentration on complex viscosity at 90°C. The results indicate that the lowering of the solution concentration also lowers the complex viscosity of the cellulose ionic liquid solution. Also, all viscosity curves show a shear-thinning effect, which is to be expected. The results for the complex

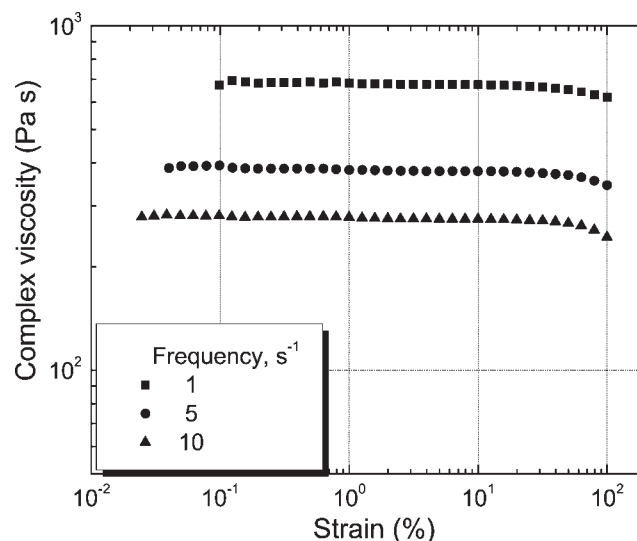


Figure 1 Dynamic strain sweep test of 10% ionic liquid solution at 80°C.

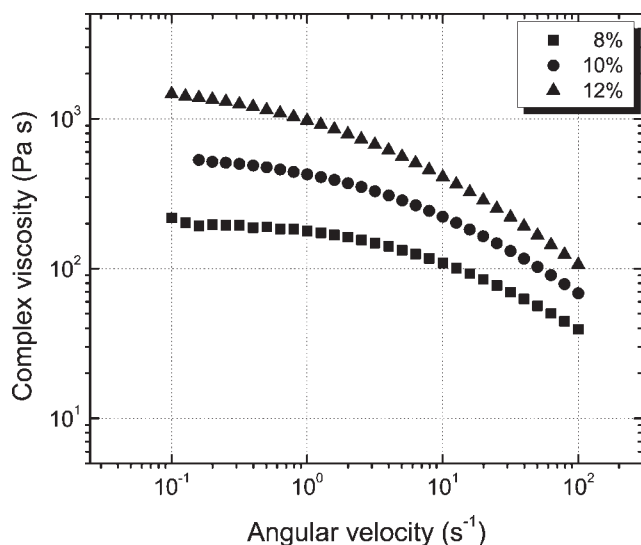


Figure 2 Complex viscosity data for all solution concentrations at 90°C.

viscosity at 80°C and 100°C are not illustrated but they display the same pattern as the 90°C solutions, where the viscosity curves are at higher and lower values for 80°C and 100°C, respectively.

The complex viscosity of cellulose ionic liquid solutions at different concentration of cellulose is compared in Figure 3 with the viscosity of a lyocell solution (cellulose dissolved in *N*-methyl-morpholine oxide monohydrate) and three melt blowing grade polypropylene melts of different viscosities, measured here by the melt flow rate (MFR in g/(10 min)). Two important features are seen by the analysis of the viscosity curves from Figure 3. First, ionic liquid solution show almost the same pattern of the viscosity curve as that of lyocell solution at the same

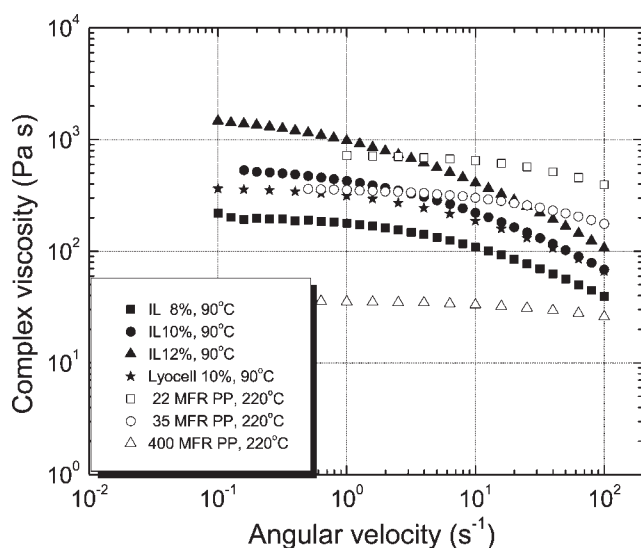


Figure 3 Complex viscosity of cellulose ionic liquid solutions, as compared with a lyocell solution and polypropylene melts of different melt flow rates.

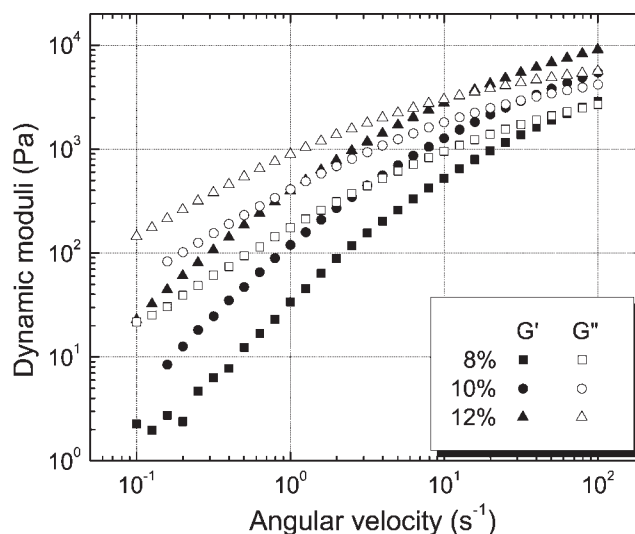


Figure 4 Dynamic moduli for all solution concentrations at 90°C.

concentration, suggesting similar set of processing parameters for spinning fibers or for making other products. Secondly, ionic liquid solution, like lyocell solutions, might be processed by the solution blowing technique to manufacture cellulosic nonwoven products, in a similar way with melt blowing of polypropylene or other polymeric melts. Literature reviews, research papers, and patent applications have already demonstrated the potential to produce, directly from lyocell solutions by melt blowing process, a wide range of cellulose web products.^{15–22}

Dynamic moduli

Dynamic moduli for solutions of different concentration in cellulose at 90°C are shown in Figure 4. As expected, the viscoelastic characteristics of the ionic liquid solutions change as the concentration changes. At low concentration the solution behaves as a viscous fluid up to the crossover point of 77 s⁻¹, as compared with solution at the highest concentration of 12%, for which the viscous domain narrowed with the corresponding widening of the elastic domain from high angular velocities down to as low as 14 s⁻¹. The viscoelastic properties are also affected by the solution temperature. The crossover point coordinate shifts to lower values as the temperature of the solution is lowered. A similar behavior of the effect of temperature and concentration was noticed in our studies on the shear rheology of lyocell solutions from different lignocellulosic materials at different concentrations.²³

Temperature shifting of complex viscosity and dynamic moduli curves

The technique of reduced variables is used here to generate master curves for shear viscosity and

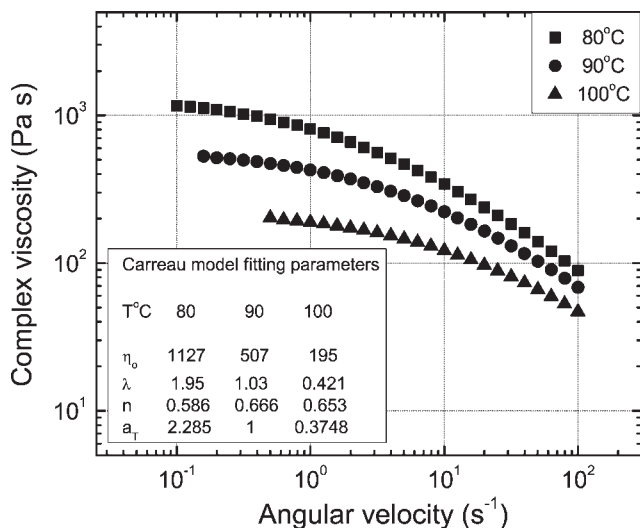


Figure 5 Complex viscosity curves and Carreau model fitting results for 10% solution.

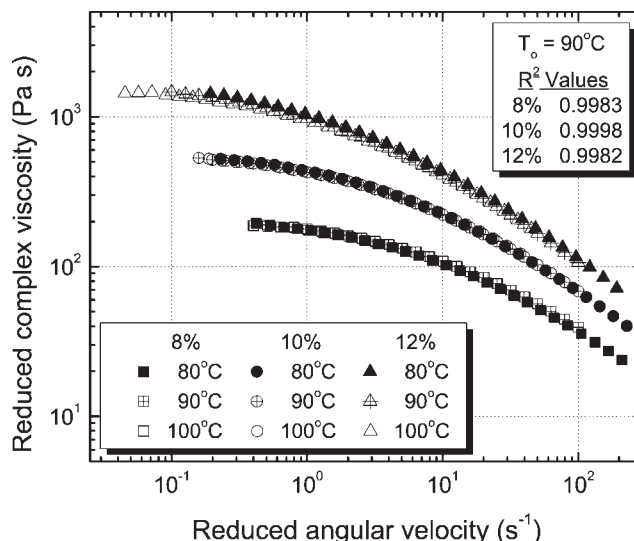


Figure 6 Master curves for complex viscosity (Carreau model parameters).

dynamic moduli.²⁴ The temperature shift factor can be defined by the following equation

$$a_T = \frac{\eta_0(T)T_0}{\eta_0(T_0)T} \quad (1)$$

where $\eta_0(T)$ and $\eta_0(T_0)$ are zero-shear viscosities of the cellulose/IL solutions at temperature T and reference temperature T_0 , respectively. Based on this shift factor, the reduced complex viscosity and reduced angular velocity are calculated with eqs. (2) and (3)

$$\eta_r^* = \eta^*(\omega, T) \frac{\eta_0(T_0)}{\eta_0(T)} = \eta^*(\omega, T) \frac{T_0}{a_T T} \quad (2)$$

$$\omega_r = \omega a_T. \quad (3)$$

Assuming that the Cox-Merz rule²⁵ is valid for the cellulose/IL solution rheology, the three-parameter Carreau and Cross viscosity models^{24,26} are used to predict the zero-shear viscosity from the complex viscosity data. The three-parameter Carreau viscosity model is given by eq. (4)

$$\eta = \eta_0 \left[1 + (\lambda \dot{\gamma})^2 \right]^{(n-1)/2} \quad (4)$$

and the three-parameter Cross model given by eq. (5)

$$\eta = \frac{\eta_0}{1 + (\lambda \dot{\gamma})^{1-n}} \quad (5)$$

where λ is a time constant and n is the power-law exponent. From the “Arrhenius type dependence” of a_T as a function of temperature, the activation energy for shear flow is determined with eq. (6)

$$a_T = \exp \left[\frac{\Delta E_a}{R} \left(\frac{1}{T} - \frac{1}{T_0} \right) \right] \quad (6)$$

where ΔE_a is the activation energy and R is the universal gas law constant.

Figure 5 shows the complex viscosity curves for the 10% solution at all tested temperatures and the Carreau model fitting parameters in the inset.

Changing the testing temperature brings about only a change in zero-shear viscosity, without modifying the general pattern of shear thinning shown for all viscosity curves. Figure 6 displays the master curves for each concentration. These curves were obtained by shifting the complex viscosity curves at 80 and 100°C on the reference viscosity curve at

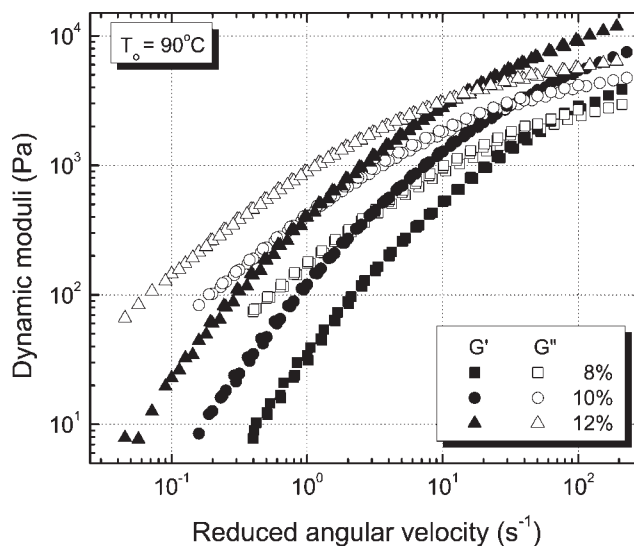


Figure 7 Master curves for the dynamic moduli of all solution concentrations (Carreau model).

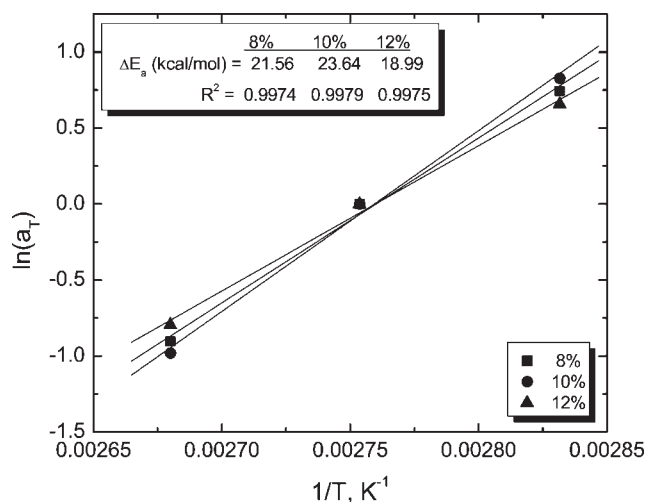


Figure 8 Arrhenius plot for the shift factors of all solution concentrations (Carreau model).

90°C. Similarly, master curves of dynamic moduli of the 8, 10, and 12% solutions were also generated using the same shift factors and shown in Figure 7. Both complex viscosity and dynamic moduli master curves show an excellent shifting accuracy, as seen from the values of the coefficient of determination R^2 . The Arrhenius plot of $\ln(a_T)$ versus $1/T$ is shown in Figure 8. From the slope of the linear fit, the activation energy for each solution concentration was calculated and is shown in the inset of the figure.

The three-parameter Cross model, like the Carreau model was also used to fit the complex viscosity data of the 8, 10, and 12% solutions at each temperature. The shift factors were again calculated using eq. (1). The fitted results are presented in Figures 9–12 in the same way as the results from the Carreau model. It can be seen from Figures 5 and 9 that Car-

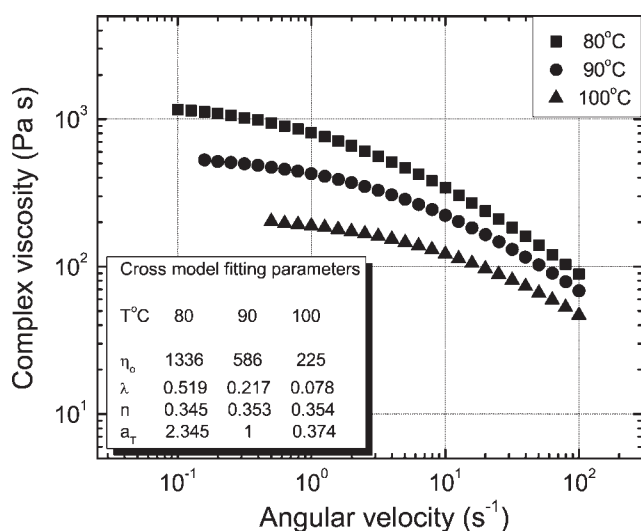


Figure 9 Complex viscosity data and Cross model fitting results for a 10% solution.

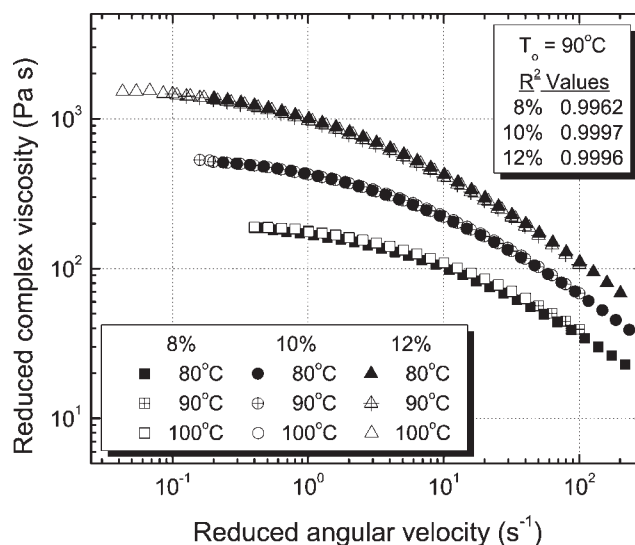


Figure 10 Shifted curves for complex viscosity for all solution concentrations (Cross model).

reau model under-predict the zero-shear viscosity, as compared with Cross model, a fact that was also observed by Carreau et al.²⁷ From Figures 6, 7, 10, and 11, it can be observed that both Carreau and Cross models yield good shifted curves for the complex viscosity and dynamic moduli. This can also be shown by the high coefficient of determination (R^2) values determined from polynomial fits of shifted complex viscosity curves, all of which were higher than 0.996. The results are summarized in Table II. The shift factors also show good Arrhenius dependence. From the slope of the Arrhenius plots, the activation energy for shear flow was calculated for each solution concentration. The results are summarized in Table III. The maxima in activation energy at 10%

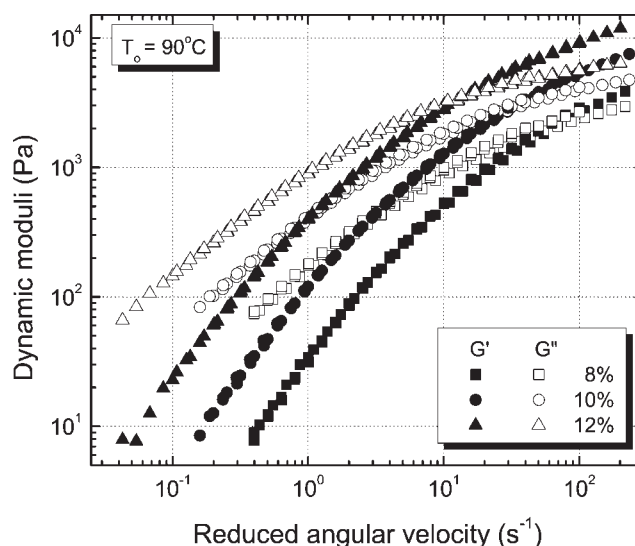


Figure 11 Shifted curves for the dynamic moduli for all solution concentrations (Cross model).

TABLE II
Coefficient of Determination (R^2) Values for the Polynomial Fits of Complex Viscosity Shift Curves Cellulose/[Bmim]Cl Solutions

Model	8%	10%	12%
Carreau	0.9983	0.9998	0.9982
Cross	0.9962	0.9997	0.9996

concentration is similar with the maxima observed by other researchers on cellulose solutions and explained by the formation of some network structures.^{28,29}

The activation energy for flow of cellulose ionic liquid solutions varies between 18.99 and 24.09 kCal/mol, being slightly higher for the Cross model. These values are almost double the activation energy of 12.9 kCal/mol, reported by our research group for a lyocell solution of 14% concentration in cellulose from a dissolving pulp of DP 855.³⁰ The activation energy for shear flow for ionic liquid solutions is even higher than the activation energy of the melt blowing grades of polypropylenes of different melt flow rates, given in Figure 3. We have calculated values of activation energy of 16.88, 12.5, and 9.82 kCal/mol for the polypropylene melts of 22, 35, and 400 MFR, respectively.³¹ All these values can be compared with the activation energies of 5.98, 14.35, and 20.33 kCal/mol, reported for polyethylene, polystyrene, and polycarbonate.²⁶

CONCLUSIONS

Complex viscosity and dynamic moduli were measured at temperatures of 80, 90, and 100°C for cellulose solutions of 8, 10, and 12 wt % dissolved in 1-butyl-3-methylimidazolium chloride and the results

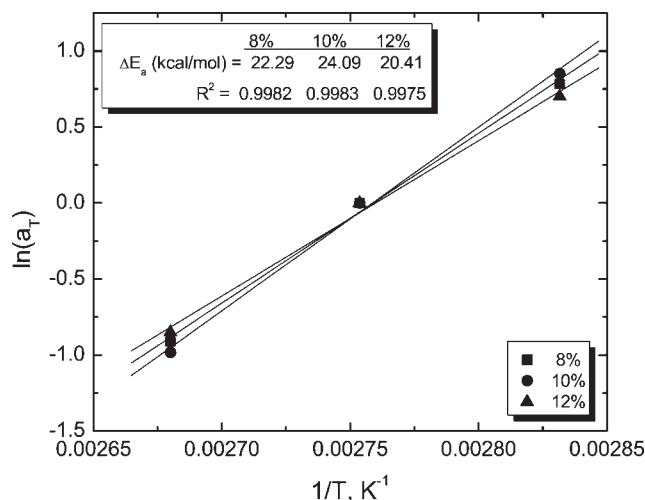


Figure 12 Arrhenius plot for the shift factors of all solution concentrations (Cross model).

TABLE III
Activation Energies for Flow and Coefficient of Determination (R^2) Values for Cellulose/[Bmim]Cl Solutions

	ΔE_a (kCal/mol)		R^2 values	
	Carreau model	Cross model	Carreau model	Cross model
8%	21.56	22.29	0.9974	0.9982
10%	23.64	24.09	0.9979	0.9983
12%	18.99	20.41	0.9975	0.9975

compared with lyocell solutions and melt blow grade polypropylene melts of different melt flow rates. The results show that the complex viscosity is comparable with that of lyocell solutions and melt blowing grade polypropylene, suggesting that they can be processed by spinning and solution blowing, for the manufacture of fiber and nonwoven products. The complex viscosity curves show typical shear thinning behavior. Good shift curves were generated for the complex viscosity and dynamic moduli, by using zero-shear viscosities fit with Carreau and Cross viscosity models. Also, activation energy for shear flow was calculated from the Arrhenius plots of shift factors at different temperatures. Activation energies between 18.99 and 24.09 kCal/mol were obtained, depending on the solution concentration and viscosity model used to fit experimental data. These values are higher than the activation energies of lyocell solutions and different polyolefin melts and comparable with those for polycarbonate melts.

References

- Seddon, K. R. *J Chem Tech Biotech* 1997, 68, 351.
- Remsing, R. C.; Swatloski, R. P.; Rogers, R. D.; Moyna, G. *Chem Commun* 2006, 1271.
- Swatloski, R. P.; Spear, S. K.; Holbrey, J. D.; Rogers, R. D. *J Am Chem Soc* 2002, 124, 4974.
- Novoselov, N. P.; Sashina, E. S.; Petrenko, V. E.; Zaborsky, M. *Fiber Chem* 2007, 39, 153.
- Massonne, K.; D'Andola, G.; Stegmann, V.; Mormann, W.; Wezstein, M.; Leng, W. *PCT Int Appl* 2007, WO 2007101811.
- Massonne, K.; D'Andola, G.; Stegmann, V.; Mormann, W.; Wezstein, M.; Leng, W.; Freyer, S. *PCT Int Appl* 2007, WO 2007101812.
- Poplin, J. H.; Swatloski, R. P.; Holbrey, J. D.; Spear, S. K.; Metlen, A.; Gratzel, M.; Nazeeruddin, M. K.; Rogers, R. D. *Chem Commun (UK)* 2007, 20, 2025.
- Turner, M. B.; Spear, S. K.; Holbrey, J. D.; Rogers, R. D. *Biomacromolecules* 2004, 5, 1379.
- Zhu, S.; Wu, Y.; Chen, Q.; Yu, Z.; Wang, C.; Jin, S.; Ding, Y.; Wu, G. *Green Chem* 2006, 8, 325.
- El Seoud, O. A.; Koschella, A.; Fidale, L. C.; Dorn, S.; Heinze, T. *Biomacromolecules* 2007, 8, 2629.
- Zhang, H.; Wang, Z.; Zhang, Z.; Wu, J.; Zhang, J.; He, J. *Adv Mater* 2007, 19, 698.
- Liu, L.-Y.; Chen, H.-Z. *Xianweisu Kexue Yu Jishu* 2006, 14, 8.

13. Collier, J. R.; Romanoschi, O.; Petrovan, S. *J Appl Polym Sci* 1998, 69, 2357.
14. Fredlake, C. P.; Crosthwaite, J. M.; Hert, D. G.; Aki, S. N. V. K.; Brennecke, J. F. *J Chem Eng Data* 2004, 49, 954.
15. Hayhurst, M. *J Chem Fibers Int* 2006, 56, 386.
16. Tang, S.; Lam P.; Mukhopadhyay, S. K. *J Text Inst* 2006, 97, 39.
17. Tang, S.; Lam P.; Law, S. J.; Mukhopadhyay, S. K. *J Text Inst, Part 1: Fibre Sci Text Technol* 2001, 92, 349.
18. Zhao, R.; Schwarz, E. C. A. U.S. Pat. Appl. Publ. CODEN: USXXCO US 2005056956 A1 20050317 (2005).
19. Luo, M.; Neogi, A. U.S. Pat. Appl. Publ. CODEN: USXXCO US 2004207110 A1 20041021 (2004).
20. Luo, M.; Roscelli, V. A.; Camarena, S.; Neogi, A. N.; Selby, J. S. *PCT Int. Appl. CODEN: PIXXD2 WO 2001081664 A1 20011101* (2001).
21. Luo, M.; Roscelli, V. A.; Camarena, S.; Neogi, A. N.; Yancey, M. J.; Gaddis, P. G. U.S. Pat. Appl. Publ. CODEN: USXXAM US 6306334 B1 20011023 (2001).
22. Steindl, T.; Einzmann, M.; Rahbaran, S.; Schmidtbauer, J.; Voglauer, B. *PCT Int. Appl. CODEN: PIXXD2 WO 2007124522 A1 20071108* (2007).
23. Dever, M.; Collier, B. J.; Petrovan, S.; Collier, J. R. *Cloth Text Res J* 2003, 21, 167.
24. Bird, R. B.; Curtiss, C. F.; Armstrong, R. C.; Hassager, O. *Fluid Mechanics*, 2nd ed.; Wiley: New York 1987; Vol. 1.
25. Cox, W. P.; Merz, E. H. *J Polym Sci* 1958, 118, 619.
26. Macosko, C. W. *Rheology: Principles, Measurements, and Applications*; Wiley-VCH: New York, Chichester, 1994.
27. Carreau, P. J.; De Kee, D. C. R.; Chabra, R. P. *Rheology of Polymeric Systems. Principles and Applications*; Hanser: New York, 1997.
28. Bumbu, G. G.; Eckelt, J.; Wolf, B. A.; Vasile, C. *Macromol Biosci* 2005, 5, 936.
29. Yang, Q.; Sheng, X.; Tan, Z.; He, X. *Xianweisu Kexue Yu Jishu* 2006, 14, 27.
30. Petrovan, S.; Collier, J. R.; Morton, J. H. *J Appl Polym Sci* 2000, 77, 1369.
31. Petrovan, S.; Collier, J. R. unpublished results.